Miscibility and Morphology of Blends of Isotactic and Atactic Poly(3-hydroxybutyrate)

Hideki Abe and Yoshiharu Doi*

Polymer Chemistry Laboratory, The Institute of Physical and Chemical Research (RIKEN), Hirosawa, Wako-shi, Saitama 351-01, Japan

Michael M. Satkowski and Isao Noda

The Procter and Gamble Company, Miami Valley Laboratories, P.O. Box 398707, Cincinnati, Ohio 45239-8707

Received July 7, 1993; Revised Manuscript Received October 18, 1993®

ABSTRACT: The spherulitic and lamellar morphology of binary blends of microbial isotactic poly[(*R*)-3-hydroxybutyrate] (P[(*R*)-3HB]) ($\bar{M}_n$ = 650 000) and synthetic atactic poly[(*R,S*)-3-hydroxybutyrate] (P[(*R,S*)-3HB]) ($\bar{M}_n$ = 56 000 and 3400) were investigated by means of optical microscopy and small-angle X-ray scattering (SAXS). The spherulites of isotactic P[(*R*)-3HB] were volume-filled, indicating the inclusion of P[(*R,S*)-3HB] within the spherulites. The radial growth rate of P[(*R*)-3HB] spherulites decreased with increased content of P[(*R,S*)-3HB]. The SAXS data show that the lamellar periodicity of P[(*R*)-3HB] increased with the content of P[(*R,S*)-3HB]. The decrease in overall crystallinity of the blend was fully accounted for by addition of the amorphous P[(*R,S*)-3HB] component; i.e., the degree of crystallinity of the crystallizable component did not appear to change much by the presence of P[(*R,S*)-3HB]. These results imply that atactic P[*R,S*)-3HB] material is included in the amorphous regions between the lamellae under certain crystallization conditions.

Introduction

A wide variety of microorganisms synthesize an optically active polymer of (*R*)-(−)-3-hydroxybutyric acid and accumulate it as a reserve energy source.[1,2] Poly[(*R*)-3-hydroxybutyrate] (P[(*R*)-3HB]) isolated from such microorganisms is a biodegradable and biocompatible thermoplastic with a melting temperature around 180 °C.[3,4] Consequently, microbial P[(*R*)-3HB] has attracted attention as an environmentally degradable resin to be used for a wide range of agricultural, marine, and medical applications.[5] Practical use of P[(*R*)-3HB] in these applications has been impeded by a number of property deficiencies. Excessive brittleness in melt crystallized films is one such undesirable attribute of P[(*R*)-3HB]. This brittleness is believed to be caused by the growth of cracks within large spherulites of P[(*R*)-3HB]. Attempts have been made to decrease the brittleness of P[(*R*)-3HB] by blending with other polymers[6–13] or acylglycerols.[14] In a previous paper,[15] we reported the physical properties and enzymatic degradability of blends of microbial isotactic P[(*R*)-3HB] with atactic synthetic P[(*R,S*)-3HB]. The atactic polymer was synthesized by ring-opening polymerization of racemic β-butyrolactone using $Zn(C_2H_5)_2/H_2O$ as a catalyst.[16] The elongation to break of the blend films increased from 5 to 200% upon the addition of 25 wt % P[(*R,S*)-3HB], and the rate of enzymatic degradation increased by 4 times. The wide-angle X-ray scattering (WAXS) data of blends suggested that the atactic P[(*R,S*)-3HB] did not cocrystallize with the isotactic P[(*R*)-3HB]. Recently, Marchessault et al.[17] studied the effect of composition of the blends of P[(*R*)-3HB] with partially and fully atactic P[(*R,S*)-3HB] on the melting temperatures. They demonstrated that there was cocrystallization between partially atactic and fully isotactic materials. Fully atactic P[(*R,S*)-3HB] did not cocrystallize with isotactic P[(*R*)-3HB].

In blend systems such as P[(*R*)-3HB]/P[(*R,S*)-3HB], there are several possible types of morphologies that may arise due to phase separation upon crystallization of one of the components. If cocrystallization does not occur and the components are miscible in the melt, then there are at least three possibilities. In the case of the macrophase-separated blend, the noncrystallizing component may be excluded from the growing spherulites of crystallizing material and be located in excess at the spherulitic boundaries. It is also possible that the noncrystallizable entity may be included within the spherulite but primarily present in amorphous regions not between individual lamellae, but rather in interfibrillar regions within the spherulite. In case of strong preference for miscibility or very fast crystallization conditions, the noncrystallizable chains may also be located in the amorphous region between the individual lamellae of crystalline material.

In this paper, the solid-state structure and morphology of binary blends of isotactic P[(*R*)-3HB] with atactic P[(*R,S*)-3HB] of high and low molecular weights are studied by means of optical microscopy and small-angle X-ray scattering (SAXS). Information gained with these techniques can determine the extent of segregation upon the crystallization of the isotactic component.

Experimental Section

Materials. The isotactic P[(*R*)-3HB] sample was produced by *Alcaligenes eutrophus* from fructose and purified by precipitation in hexane from chloroform solution at room temperature.[18] The atactic P[(*R,S*)-3HB] was prepared by ring-opening polymerization of racemic β-butyrolactone in the presence of the $Zn(C_2H_5)_2/H_2O$ catalyst.[19] The polymerization of racemic β-butyrolactone with $Zn(C_2H_5)_2/H_2O$ catalyst was carried out in 1,2-dichloroethane at 60 °C for 5 days. The isotactic dyad fraction of the polymer was 0.51, which was determined by analysis of the 125-MHz ^{13}C NMR spectrum. The molecular weights of the P[(*R*)-3HB] and P[(*R,S*)-3HB] samples are summarized in Table 1.

Preparation of Blends. Blend films of P[(*R*)-3HB] with P[(*R,S*)-3HB] were prepared by conventional solvent-casting techniques from chloroform solution using glass Petri dishes as casting surfaces. The films were then aged for at least 3 weeks at room temperature to reach equilibrium crystallinity prior to analysis.[20]

® Abstract published in *Advance ACS Abstracts*, December 1, 1993.

0024-9297/94/2227-0050$04.50/0

Table 1. Molecular Weights of P[(*R*)-3HB] and P[(*R,S*)-3HB] Samples, Determined by GPC

sample	$\bar{M}_n$	$\bar{M}_w/\bar{M}_n$
P[(*R*)-3HB]	650 000	1.8
P[(*R,S*)-3HB] (56 000)	56 000	1.3
P[(*R,S*)-3HB] (3400)	3 400	2.5

Analytical Procedures. All molecular weight data were obtained by gel-permeation chromatography at 40 °C, using a Shimadzu 6A GPC system and 6A refractive index detector with Shodex K-80M and K-802 columns. Chloroform was used as eluent at a flow rate of 0.8 mL/min, and sample concentrations of 1.0 mg/mL were applied. Polystyrene standards with a low polydispersity were used to make a calibration curve.

The morphologies of P[(*R*)-3HB] spherulites were observed with a Zeis optical microscope equipped with crossed polarizers and a Linkham hot stage. The films (2 mg) of P[(*R*)-3HB]/P[(*R,S*)-3HB] blends, as obtained by solvent casting, were first heated on a hot stage from room temperature to 190 °C at a rate of 30 °C/min. Samples were maintained at 190 °C for 2 min, and then the temperature was rapidly lowered to a desired crystallization temperature (T_c). The samples were crystallized isothermally at a given T_c to monitor the growth of the spherulites as a function of time. The radial growth rate of P[(*R*)-3HB] spherulites was calculated as the slope of the line obtained by plotting the spherulite radius against time. During the thermal treatment, the blend films were kept under nitrogen flow to limit the degradation of the polymer. We recognize that exposure of PHB to excessive temperature results in molecular weight reduction. The molecular weights of the melt crystallized samples are indeed slightly lower than the starting conditions. GPC data collected on samples treated with these thermal histories indicated that PHB tends to have its molecular weight decreased by no more than 20%. By applying uniform heating/cooling profiles and with minimal exposure of PHB to temperatures above 140 °C, the extent of the decomposition was reduced. All molecular weights given are those preceding melt treatment.

The lamellar periodicities of P[(*R*)-3HB] were determined from the small-angle X-ray scattering (SAXS) patterns. Samples (3 mm thick) were isothermally crystallized at 90 °C for at least 1 day after melting at 190 °C for 2 min. Radiation of wavelength 0.154 nm (Cu Kα) was employed. Sample exposure times ranged between 1 and 4 h at a generator power of 40 kV and 60 mA. X-rays were collimated by an Anton Parr compact Kratky device with slit width set at 30 μm. A position-sensitive detector was used to measure scattered intensities. Raw data patterns were corrected for background scattering and absorption but not for slit smearing. In addition, the scattering due wide-angle diffraction was also subtracted from the patterns. This wide-angle correction amounted to fitting the innermost part of the amorphous halo at higher angles (>6°) to the form suggested by Vonk[21] and subtracting this fitted profile from the patterns.

Results and Discussion

Spherulite Morphology. The P[(*R*)-3HB] spherulites were observed with a polarized optical microscope as a function of time at a given temperature for various compositions of P[(*R*)-3HB]/P[(*R,S*)-3HB] blends. In this study, two samples of atactic P[(*R,S*)-3HB] of different molecular weights, $\bar{M}_n$ = 3400 and 56 000, were used. Figure 1 shows typical micrographs of spherulites for the blends of P[(*R*)-3HB] with P[(*R,S*)-3HB] ($\bar{M}_n$ = 56 000). The samples were isothermally crystallized at a temperature between 85 and 120 °C after melting at 190 °C for 2 min. The addition of atactic P[(*R,S*)-3HB] affects the texture of the spherulite significantly at 50% composition. Figure 1 shows an increase in fibrous texture and less obvious banding when the composition of P[(*R,S*)-3HB] is increased from 25 to 50%. There was no evident slowing of the growth fronts as the spherulites impinge. The spherulite radius increased linearly with time. The radial growth rate was dependent on both the crystallization temperature and the blend composition. After crystallization, the spherulites were well-developed throughout the blend films, and no apparent evidence of phase separation of noncrystalline P[(*R,S*)-3HB] was detected, even at the highest concentrations studied (50 wt %). These results indicate that the atactic component exists within the spherulites of P[(*R*)-3HB]. Similar observations were made by Marchessault et al.[17] on the blends of completely atactic P[(*R,S*)-3HB] and isotactic P[(*R*)-3HB] cast from solution mixtures.

Figure 2 shows the radial growth rate (G) of P[(*R*)-3HB]/P[(*R,S*)-3HB] blend spherulites at different crystallization temperatures for blends with P[(*R,S*)-3HB] of

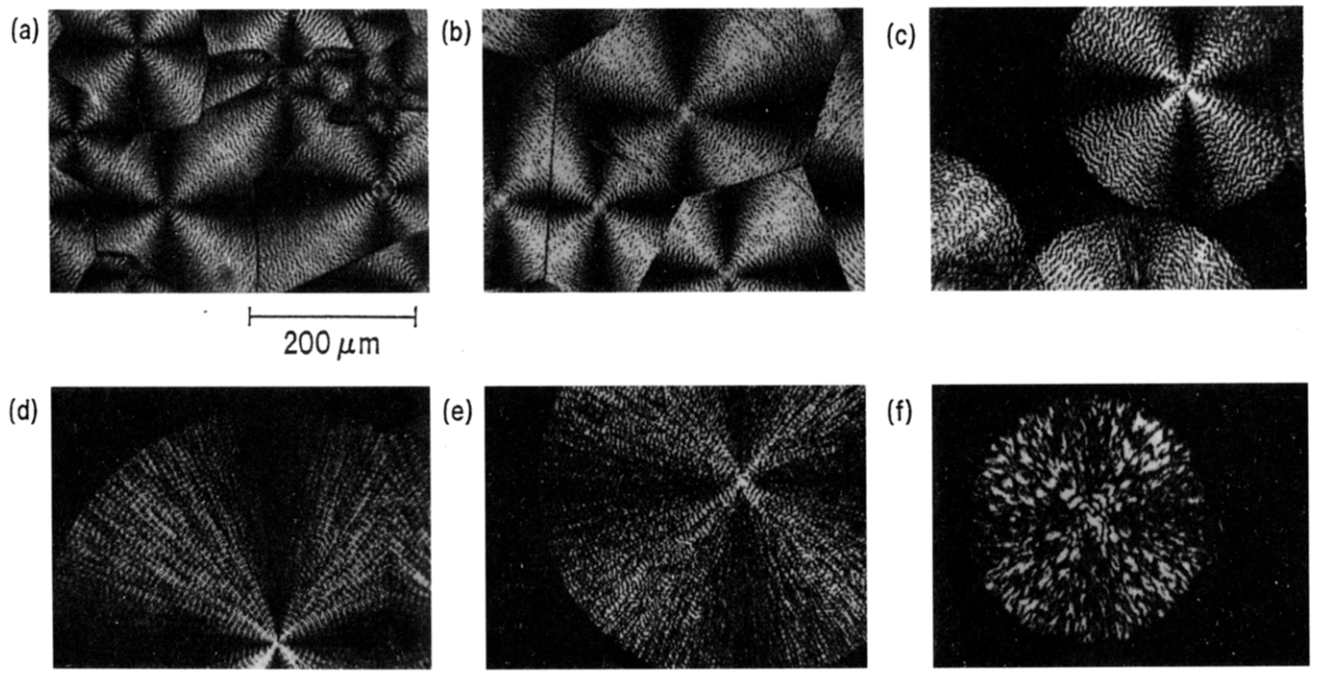

Figure 1. Optical micrographs of P[(*R*)-3HB] spherulites of P[(*R*)-3HB]/P[(*R,S*)-3HB] blends with P[(*R,S*)-3HB] component molecular weight 56 000. (a) P[(*R*)-3HB]/P[(*R,S*)-3HB] (75:25 w/w) after completion of crystallization at T_c = 85 °C, (b) (75:25 w/w) after completion of crystallization at T_c = 110 °C, (c) (75:25 w/w) during growth at T_c = 120 °C, (d) (50:50 w/w) during growth at T_c = 85 °C, (e) (50:50 w/w) during growth at T_c = 95 °C, and (f) (50:50 w/w) during growth at T_c = 120 °C.

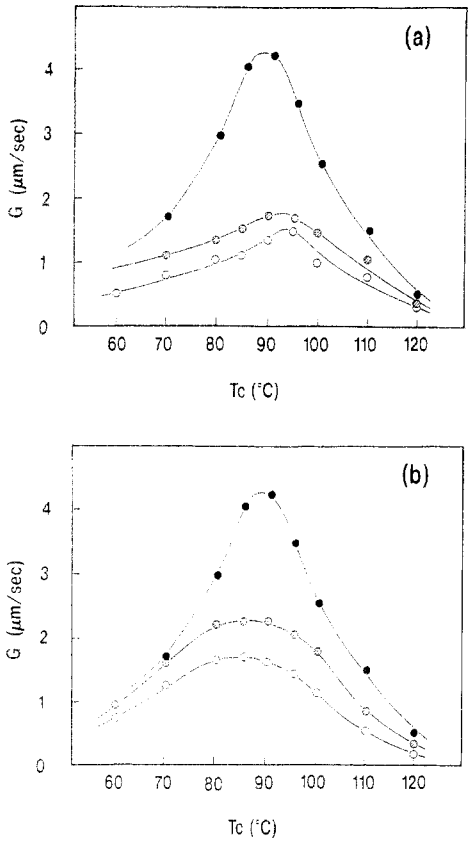

Figure 2. Radial growth rate (G) of P[(R)-3HB] spherulites at various crystallization temperatures (T_c) for (a) P[(R)-3HB]/P[(R,S)-3HB] (56 000) blends and (b) P[(R)-3HB]/P[(R,S)-3HB] (3400) blends of different compositions (w/w): 100/0 (●), 75/25 (⊘), 50/50 (○).

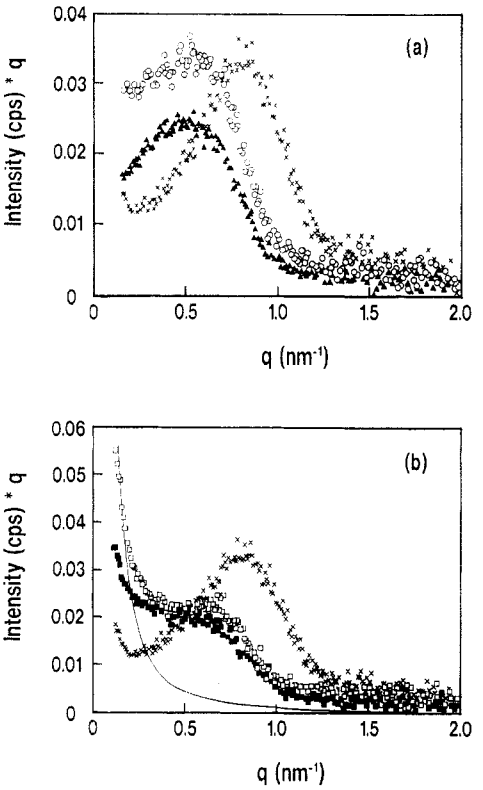

Figure 3. Variation in relative small-angle X-ray scattering (SAXS) intensity with q: (a) pure P[(R)-3HB] (×), P[(R)-3HB]/P[(R,S)-3HB] (56 000) (75:25 w/w) blend (○), and P[(R)-3HB]/P[(R,S)-3HB] (3400) (75:25 w/w) blend (▲); (b) pure P[(R)-3HB] (×), P[(R)-3HB]/P(R,S)-3HB] (56 000) (50:50 w/w) blend (□), and P[(R)-3HB]/P[(R,S)-3HB] (3400) (50:50 w/w) blend (■).

$\bar{M}_n$ = 56 000 and 3400, respectively. A maximum value (4.31 μm/s) of G was observed near 90 °C for P[(R)-3HB] homopolymer. The G values decreased with increased content of atactic P[(R,S)-3HB]. The temperature of peak growth rate is largely unaffected since addition of atactic P[(R,S)-3HB] does not decrease the glass transition of the blend very much. There is little melting point depression of the crystallizable component observed in these blends, which is in agreement with the findings of Pearce et al.[17] The small changes in T_g and T_m of the blends result in approximately the same observed temperature for maximum crystallization rate for blends as the pure polymer.

It should be noted that little observable T_m depression in this system does not preclude miscibility. Melting point depression in systems such as these are expected to vary only slightly, on the order of few degrees. The equation for melting point depression based on Flory–Huggins theory for polymer blends can be written as[22,23]

$$\frac{1}{T_m} - \frac{1}{T^0_m} = -\frac{RV_2}{\Delta H^0 V_1}\left[\frac{\ln(1-\Phi_1)}{n_2} + \left(\frac{1}{n_2} - \frac{1}{n_1}\right)\Phi_1 + \chi_{12}\Phi_1^2\right] \quad (1)$$

where T_m and T^0_m are the equilibrium melting points of the blend and homopolymer, V_2 and V_1 are the molar volumes of the repeat units of the crystallizing and noncrystallizing polymer, ΔH^0 is the heat of fusion of 100% crystalline polymer, n_2 and n_1 are degrees of polymerization of the crystalline and noncrystalline polymer, Φ_1 is the volume fraction of the crystallizable polymer, and χ_{12} is the Flory interaction parameter. In the isotactic P[(R)-3HB]/atactic P[(R,S)-3HB] blend studied here, the molecular weights are rather high, leading to small contributions for the first two terms in brackets. The interaction parameter in this case iis also expected to be very small since no strong specific molecular interactions are present. As an example, melting point depression in the case of an analogous system, isotactic polystyrene (iso-PS)/atactic polystyrene (ata-PS), is less than 3 °C in 60:40 iso-PS/ata-PS blends with molecular weight of both components near 500 000.[24] In fact, large (>5 °C) melting point depressions are observed only in low molecular weight ($\bar{M}_w$ = 900) ata-PS components at atactic volume fractions above 50%. Consequently, the spherulitic growth rate curves of iso-PS/ata-PS blends are similar in form to those of the P[(R)-3HB]/P[(R,S)-3HB] in Figure 2a. The temperature of maximum growth rate is not depressed in the high molecular weight atactic component ($\bar{M}_n$ = 56 000), just as observed in iso-PS/ata-PS by Keith and Padden.[25] They have explained this in terms of the low mobility of larger, noncrystallizable components which consequently decrease the concentration of crystallizable species at the growth front. In contrast, the temperature of maximum growth rate is slightly shifted to lower temperatures in the blend with low molecular weight atactic component ($\bar{M}_n$ = 3400), and the growth rates are slightly larger than those of P[(R)-3HB]/P[(R,S)-3HB] (50 000) blends. These phenomena may be attributed to the higher mobility of the low molecular weight atactic component.

Lamellar Morphology. The lamellar periodicities of P[(R)-3HB] were determined by analysis of the small-angle X-ray scattering (SAXS) patterns of P[(R)-3HB]/P[(R,S)-3HB] blends. Figure 3 shows the variation in relative SAXS intensities as a function of the magnitude of the scattering vector q for the blends of P[(R)-3HB] and P[(R,S)-3HB] (56 000 or 3400). The curves are plotted

as Iq vs q. This reflects the so-called "Lorentz" correction which accounts for the isotropic nature of the lamellar system. The scattering vector magnitude is defined by $q = 4\pi\sin\theta/\lambda$, where θ is half the scattering angle and λ is the wavelength of the radiation. The lamellar periodicity (Lp) can be determined by

$$\mathrm{Lp} = 2\pi/q_{\max} \quad (2)$$

where $q_{\max}$ is the q value at a maximum SAXS intensity. In Figure 3a, the $q_{\max}$ value for pure P[(*R*)-3HB] was near 0.82 nm^{-1}. The Lp of the P[(*R*)-3HB] sample is thus 7.6 nm. The magnitude of this long period is in the range of those found by Mitomo et al.[26] for P[(*R*)-3HB]. Exact values are difficult to compare since in that study, P[(*R*)-3HB] was crystallized from solution. For the blends, the lamellar periodicity of P[(*R*)-3HB]/P[(*R*,*S*)-3HB] (56 000) (75:25 w/w) blend was 12.0 ± 1 nm, and for a blend of P[(*R*)-3HB]/P[(*R*,*S*)-3HB] (3 400) (75:25 w/w), the lamellar periodicity was calculated as 11.5 ± 1 nm. The differences are within experimental error. Adding atactic P[(*R*,*S*)-3HB] to isotactic P[(*R*)-3HB] does not increase the crystallinity of the isotactic P[(*R*)-3HB] component from DSC results. In fact, heats of fusion of the blends are nearly the same as that of pure isotactic P[(*R*)-3HB] weighted for the amount of P[(*R*)-3HB] in the blend. This observation coupled with the SAXS results suggests that atactic P[(*R*,*S*)-3HB] polymer chains are included in the amorphous region between the individual lamellae of P[(*R*)-3HB]. An increase in the lamellar periodicity of crystallizable component in the polymer blend attributable to interlamellar segregation of the second noncrystallizable component has been observed for the poly(ϵ-caprolactone) (PCL)/poly(vinyl chloride) blend[27] and PCL/poly(styrene-*co*-maleic anhydride) blend.[28]

It is interesting to contrast the P[(*R*)-3HB]/P[(*R*,*S*)-3HB] SAXS results with those of iso-PS/ata-PS. Warner et al.[29] examined the small-angle scattering of iso-PS/ata-PS blends some time ago. In that study, though the spherulites formed were volume filling, the long periods remained invariant upon addition of atactic material. The conclusion was that the amorphous component was able to diffuse away from the growing crystal front to the interfibrillar regions within the spherulite. Apparently, in P[(*R*)-3HB]/P[(*R*,*S*)-3HB] blends, some of the atactic material gets trapped between individual lamellae, causing the long period to change. The major difference between the two systems which may explain these observations is the difference in crystal growth rates. Typical growth rate for iso-PS is about 0.005 μm/s. From Figure 2 it can be seen that the growth rate of P[(*R*)-3HB is nearly 3 orders of magnitude faster than iso-PS.

In P[(*R*)-3HB]/P[(*R*,*S*)-3HB] blends there appears to be limits to this incorporation. In Figure 3b, the SAXS profiles are shown on the 50:50 w/w P[(*R*)-3HB]/P[(*R*,*S*)-3HB] blends for atactic molecular weights of 3400 and 56 000. The characteristic peak is replaced by a shoulder and a large increase in the scattering as q approaches zero, especially in the 56 000 molecular weight atactic component. This upturn in I at low angles makes assignment of a periodicity uncertain. The nature of this "zero-order" peak in crystalline polymers has been addressed by Schultz[30] and Vonk.[31] The zero-order peak arises either from large (greater than lamellae length scales) individual, independently scattering amorphous zones or from isolated (nonstacked) lamellar crystals. Vonk has tabulated the expected decay in intensity from $q = 0$ for different types of entities. For isolated lamellae measured by slit geometry, smeared data would decrease as $I \propto 1/q$. A general two-phase structure will drop in intensity as $1/q^3$. The solid line in Figure 3b is an intensity pattern corresponding to $I = \alpha/q^3$ where α is a scaling constant. This type of scattering would be produced in slit collimation for independently scattering entities at angles much greater than the inverse of radius of gyration of the entity. This result agrees with the model of large amorphous zones. Since P[(*R*)-3HB]/P[(*R*,*S*)-3HB] blend volumes fill in all cases, these large amorphous zones are present within the spherulite. If one assumes that the size scales of these amorphous zones and the lamellae are very disparate, the scattering from these two different sources would superimpose. Subtraction of the $1/q^3$ contributions would yield the scattering from the lamellae. When analyzed in this manner, the resultant periodicities are 10.5 nm for the 50:50 w/w P[(*R*)-3HB]/P[(*R*,*S*)-3HB] blend with P[(*R*,*S*)-3HB] molecular weight 56 000 and 11.5 nm for the 50:50 w/w P[(*R*)-3HB]/P[(*R*,*S*)-3HB] blend with P[(*R*,*S*)-3HB] molecular weight 3400. This is somewhat smaller than the 75:25 blend samples but still significantly larger than the P[(*R*)-3HB] alone. The nature of the assumptions involved here makes accurate calculation of long periods uncertain, but it appears as if there is still some increase of long period compared to pure P[(*R*)-3HB].

Conclusions

The spherulitic and lamellar periodicities of binary blends of microbial isotactic poly[(*R*)-3-hydroxybutyrate] (P[(*R*)-3HB]) ($\bar{M}_n$ = 650 000) and synthetic atactic poly-[(*R*,*S*)-3-hydroxybutyrate] (P[(*R*,*S*)-3HB]) ($\bar{M}_n$ = 56 000 and 3400) were investigated by means of optical microscopy and small-angle X-ray scattering (SAXS). The spherulites of isotactic P[(*R*)-3HB] grew in apparent equilibrium with one-phase melt for blends of P[(*R*)-3HB] and P[(*R*,*S*)-3HB]. The radial growth rate of P[(*R*)-3HB] spherulites decreased with increasing content of P[(*R*,*S*)-3HB] in a manner reminiscent of the classical system of iso-PS/ata-PS. In contrast to the behavior of iso-PS/ata-PS, the SAXS data showed that the interlamellar distance of P[(*R*)-3HB]/P[(*R*,*S*)-3HB] blends was greater than pure P[(*R*)-3HB]. These results indicate that atactic P[(*R*,*S*)-3HB] chains were incorporated in the amorphous regions between individual lamellae within the spherulites.

Acknowledgment. We gratefully acknowledge Prof. Keith Keefer of the University of Cincinnati for use of his laboratory's scattering facilities. We also thank Andrea Heape (Procter & Gamble) for thermal analysis measurements.

References and Notes

(1) Doi, Y. *Macrobial Polyesters*; VCH Publishers: New York, 1990.
(2) Dawes, E. A.; Senior, P. J. *Adv. Microb. Physiol.* **1973**, *10*, 135.
(3) Holmes, P. A. *Phys. Technol.* **1985**, *16*, 32.
(4) Braham, P. J.; Keller, A.; Otun, E. I.; Holmes, P. A. *J. Mater. Sci.* **1984**, *19*, 2781.
(5) King, P. P. *J. Chem. Tech. Biotechnol.* **1982**, *32*, 2.
(6) Avella, M.; Martuscelli, E. *Polymer* **1988**, *29*, 1731.
(7) Greco, P.; Martuscelli, E. *Polymer* **1989**, *30*, 1475.
(8) Yasin, M.; Holland, S. J.; Jolly, A. M.; Tighe, B. T. *Biomaterials* **1989**, *10*, 400.
(9) Kumagai, Y.; Doi, Y. *Polym. Degrad. Stab.* **1992**, *35*, 87.
(10) Kumagai, Y.; Doi, Y. *Polym. Degrad. Stab.* **1992**, *36*, 241.
(11) Kumagai, Y.; Doi, Y. *Polym. Degrad. Stab.* **1992**, *37*, 253.
(12) Azuma, Y.; Yoshie, N.; Sakurai, M.; Inoue, Y.; Chujo, R. *Polymer* **1992**, *33*, 4763.
(13) Scandola, M.; Ceccorulli, G.; Pizzoli, M. *Macromolecules* **1992**, *25*, 6441.
(14) Ishikawa, K.; Kawaguchi, Y.; Doi, Y. *Kobunshi Ronbunshu* **1991**, *47*, 221.
(15) Kumagai, Y.; Doi, Y. *Makromol. Chem., Rapid Commun.* **1992**, *13*, 179.

(16) Teranishi, K.; Iida, M.; Araki, T.; Yamashita, S.; Tani, H. *Macromolecules* **1974**, *7*, 421.
(17) Pearce, R.; Jesudason, J.; Orts, W.; Marchessault, R. H.; Bloembergen, S. *Polymer* **1992**, *33*, 4647.
(18) Kawaguchi, Y.; Doi, Y. *Macromolecules* **1992**, *25*, 2324.
(19) Tanahashi, N.; Doi, Y. *Macromolecules* **1991**, *24*, 5732.
(20) Bloembergen, S.; Holden, D. A.; Hamer, G. K.; Bluhm, T. L.; Marchessault, R. H. *Macromolecules* **1986**, *19*, 2865.
(21) Vonk, C. *Small Angle X-ray Scattering*; Glatter, O., Kratky, O., Eds.; Academic Press: New York, 1982.
(22) Flory, P. J. *Principles of Polymer Chemistry*; Cornell University Press: Ithaca, NY, 1953.
(23) Nishi, T.; Wang, T. T. *Macromolecules* **1975**, *8*, 909.
(24) Yeh, G.; Lambert, S. *J. Polym. Sci., Part A-2* **1972**, *10*, 1183.
(25) Padden, H.; Keith, F. *J. Appl. Phys.* **1964**, *35*, 1286.
(26) Mitomo, H.; Barham, P.; Keller, A. *Polym. J.* **1987**, *19*, 1241.
(27) Khambatta, F. B.; Warner, F.; Russell, T.; Stein, R. S. *J. Polym. Sci., Polym. Phys. Ed.* **1976**, *14*, 1391.
(28) Defieuw, G.; Groeninckx, G.; Reynaers, H. *Polymer* **1989**, *30*, 2158.
(29) Waner, F.; MacKnight, W.; Stein, R. *J. Polym. Sci., Polym. Phys. Ed.* **1977**, *15*, 2113.
(30) Shultz, J. M. *J. Polym. Sci., Polym. Phys. Ed.* **1976**, *14*, 2291.
(31) Vonk, C. G.; Koga, Y. *J. Polym. Sci., Polym. Phys. Ed.* **1985**, *23*, 2539.